How to Choose the Best MEMS Sensor for a Wireless Condition-Based Monitoring System—Part 2: How to Detect Mechanical Faults

Richard Anslow, IC Design Engineer and
Chris Murphy, Application Engineer

Introduction

Part 1, "How to Choose the Best MEMS Sensor for a Wireless Condition-Based Monitoring System—Part 1," of this article series introduced the Voyager wireless CbM module as well as some key features to look out for when measuring vibration wirelessly with MEMS accelerometers. Part 2 will focus on describing common AC induction motor (ACIM) faults and will detail how to identify and diagnose specific fault types as well as the advantages triaxial MEMS accelerometers can offer over other vibration sensors.

Effects of Motor and Asset Failures on Manufacturing

When a critical motor unexpectedly breaks down in a factory, production stops. If a specific part or even the entire motor needs to be replaced, there is a risk that long lead times may be incurred. Unplanned downtime costs 10 times more than planned downtime.[1] Annually, the average factory downtime is around 800 hours.[1] The net result of this information is that CbM is growing rapidly at a time when wireless technology coupled with recent advancements in MEMS sensor technology are allowing factory and maintenance managers to rapidly deploy highly effective wireless CbM systems to stem losses due to unplanned downtime. While triaxial MEMS sensors are likely to be at the heart of this wireless revolution, there is still some confusion as to what exactly these vibration sensors are capable of.

Where Do Triaxial MEMS Accelerometers Fit on the Vibration Sensor Spectrum?

To minimize production downtime, it is imperative to know about the potential failures within the motor to be ready to deal with them. While single-axis analog output MEMS sensors, designed specifically to rival piezo vibration sensors, have recently achieved similar levels of performance to low-level/mid-level piezo sensors in terms of being able to diagnose faults, this article is more focused on narrow bandwidth monitoring (0 Hz to 1 kHz) more commonly seen in triaxial MEMS accelerometers. Not every CbM deployment is focused on diagnosing or even predicting asset faults. In some assets, it may be acceptable to detect faults at a later stage, and therefore, the sensor performance and cost can be a little lower. This is where triaxial MEMS accelerometers can offer a high performance (low noise down to 25 $\mu g/\sqrt{Hz}$) and low cost alternative as shown in Figure 1. Comparing the ADXL356 and piezo sensor PZT 8, there is a 20× cost increase with very few high performance, low cost MEMS alternatives in between. Significant growth in this area is expected over the coming years.

Why Is There a Need to Detect Vibrations Below 10 Hz/600 rpm in CbM Applications?

Low frequency CbM vibration measurements are generally considered to be within a 0.1 Hz to 10 Hz or 6 rpm to 600 rpm bandwidth. Low frequency applications are more complicated than general machinery monitoring because motion below 10 Hz (600 rpm) produces very little vibration. While it is well understood that measuring high frequency vibration data with high sensitivity sensors can help to detect certain faults (bearing spalling, gear meshing, and pump cavitation) and give potential insights into the remaining useful life of an asset, it should be noted that important information is also available closer to DC or 0 Hz. For this reason, special purpose noncontact sensors like eddy current displacement or proximity probes can be used to detect motor shaft displacements or misalignments to a high degree of accuracy at 0 Hz and even high frequency vibrations, but they can be difficult to position in some applications compared to MEMS and are typically more expensive. MEMS are in no way designed to replace eddy current sensors that can detect displacements below 0.1 nm in extreme conditions.[3] However, for designers wishing to implement a low cost CbM system or even a wireless system that can detect acceleration down to 0 Hz, MEMS accelerometers can offer a cost-effective alternative.

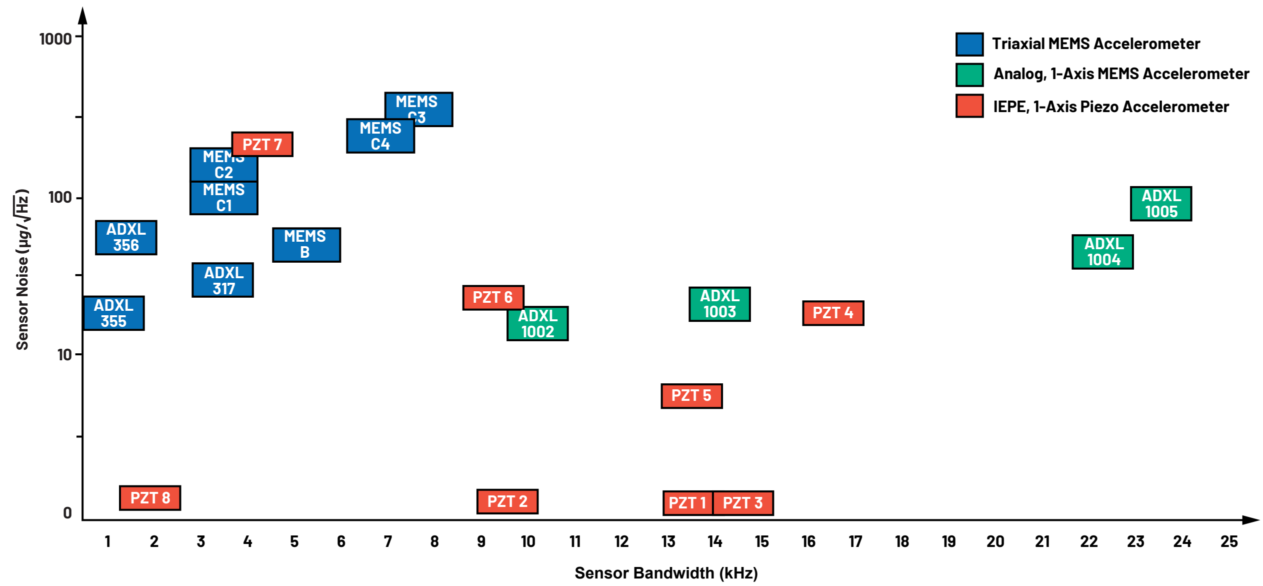

Figure 1. Triaxial MEMS sensors for CbM compared to higher performance MEMS and IEPE sensors.

Industries like paper and pulp processing, food and beverage, oil and gas, wind turbine power generation, and metal processing and mining all use very low speed motors at speeds lower than 1 Hz; therefore, it is critical for a vibration sensor to be able to detect these fundamental rpm speeds, especially when trying to detect imbalance and misalignment faults. Specialized low frequency IEPE or piezo sensors with a frequency response starting from 0.1 Hz are available while general-purpose sensors starting from 2 Hz to 5 Hz are more common. One key advantage of MEMS over piezo sensors is the fact they can detect down to 0 Hz yielding tilt information. This is not possible to test on a modal shaker, so measurements are limited to 0.01 Hz as shown in Figure 2. It should be noted that the piezo sensor is significantly more expensive and, as expected, has a better noise performance from just under 0.1 Hz upward, but below this, the MEMS sensor has better noise performance down to 0.01 Hz and on to 0 Hz. This low frequency performance is a feature on all axes of multiaxis MEMS accelerometers, potentially giving maintenance and facilities engineers further insights into the low frequency dynamics of their assets previously not possible even with highly specialized piezo sensors.

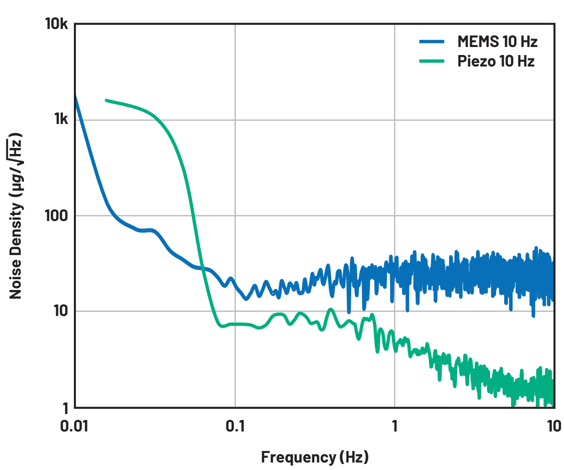

Figure 2. MEMS vs. piezo low frequency response.

Typically, it is recommended the frequency response of the accelerometer should be 40 to 50 times the shaft rpm for bearing monitoring and up to 5 times the blade pass frequency for fans and gearboxes.[4] Very slow speed machinery such as paper machine rollers, screw conveyors, and stone crushing equipment all have roller element bearings. Rpm speeds on some machines may be as low as 0.2 Hz or 12 rpm.[5] 1×, 2×, and 3× rpm speed information are vital in detecting and diagnosing imbalance, misalignment, and mechanical looseness. Stamping machine crank bearings may operate as low as 0.18 Hz or 11 rpm.[5] For wireless CbM systems, eddy current sensors are not yet viable due to their high power consumption. MEMS accelerometers offer a lower performance, lower cost alternative to multimodal vibration, and displacement measurements based on the piezo accelerometers and eddy current probes.

Using Voyagers Triaxial MEMS Accelerometer to Detect Soft Foot or Tilt Issues

ACIMs can vary in size and power with some larger motors requiring rigid foundations as shown in Figure 3. A typical application is industrial pumps where power is transferred from the shaft to the pump via a direct connection or some coupling element. Misalignment of these connections can be radial, axial, or tangential. To maintain stable alignment, vibrations must be minimized by securing the pump to a solid foundation. A stable, rigid foundation with uniform stiffness can improve reliability by reducing vibrations, effectively extending the lifetime of a motor. Industrial pumps are typically bolted directly to a machined baseplate, with accompanying equipment aligned and fixed to the same baseplate. The assembly is then adhered to a concrete foundation.

If a foundation is too flexible or uneven, this can lead to alignment issues, increased vibration magnitudes, and ultimately unplanned downtime. Alignment tests are carried out when a motor is installed and in the initial phase of operation, after maintenance or repair works, and during scheduled maintenance. Various mechanical devices can be used to detect misalignment such as feeler gauges, calipers, and dial indicators. Alternative tools such as laser alignment systems are widely used to align motor shafts and the equipment they drive.

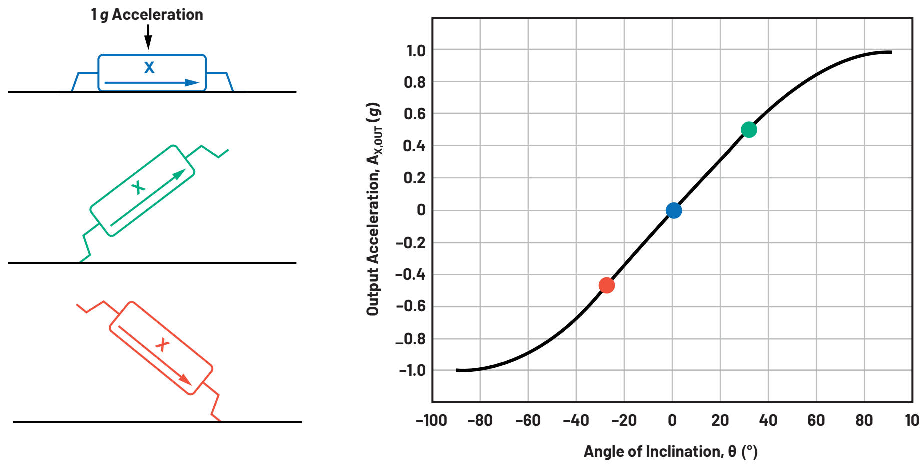

Figure 4. MEMS accelerometer with sensitive axis perpendicular to 1 g.

Once operational, routine maintenance checks will look for any anomalies with the motor to foundation alignment or motor mounting, but these could be months apart. Current maintenance regimes rely on vibration data to detect imbalance and misalignment and have proved successful for decades. Under low *g* conditions, MEMS triaxial sensors can continuously monitor and detect vibration and tilt changes, which, when combined, can provide extra confidence in measurements and potentially earlier fault detection.

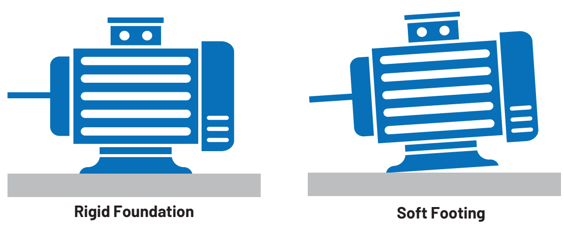

Figure 3. Soft foot is a common issue when aligning rotating equipment.

How Do MEMS Accelerometers Measure Tilt?

When a single-axis accelerometer is placed flat on a surface, as shown in Figure 4, its sensitive axis is perpendicular to gravity and therefore outputs 0 *g*. When the sensor is tilted in the direction of gravity, it detects acceleration due to the 1 *g* field. The slope of the curve in Figure 4 is the sensitivity of the device. Note the sensitivity decreases as the angle between the horizon and the x-axis increases.

In Figure 5, we can see the Voyager module measuring acceleration due to gravity or static acceleration. The module is placed upright with 1 *g* of acceleration in the z-axis and 0 *g* in the x- and y-axes. When the Voyager module is tilted 4° in the x-axis, at 22 s, the tilt can be easily observed as shown in Figure 5 as a DC offset. Converting the measured acceleration to a tilt angle involves taking the inverse sin of the measured acceleration $\sin^{-1} 0.07\ g = 4°$.

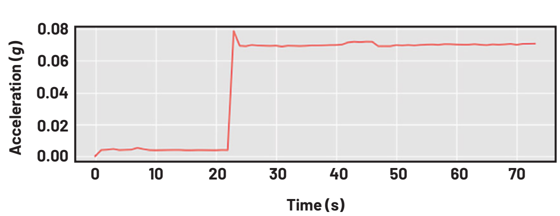

Figure 5. Voyager module detecting 4° of the tilt under static conditions.

Several issues arise when detecting the tilt under vibration for a CbM application. First, it is more difficult and requires more consideration compared to static conditions. Second, the tilt or inclination applications typically limit bandwidth to reduce noise (<100 Hz), whereas in CbM a wider bandwidth (1 kHz or higher) is favored. An extreme range to detect the tilt of an asset or motor might be limited to ±5° or ±87 m*g*, as shown in Figure 6, which can be considered a challenge in the potential presence of high *g* vibrations.

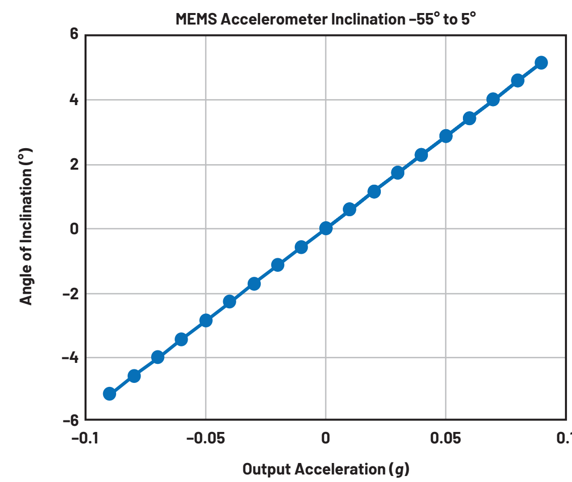

Figure 6. Output acceleration vs. angle of inclination under static conditions.

Applying a trigonometric function to the measured acceleration can easily yield the angle of inclination. However, if a shock event or vibration is detected, this can affect the inclination measurement as shown in Figure 7 where a 2 *g* impact event yields an inclination value of 82°.

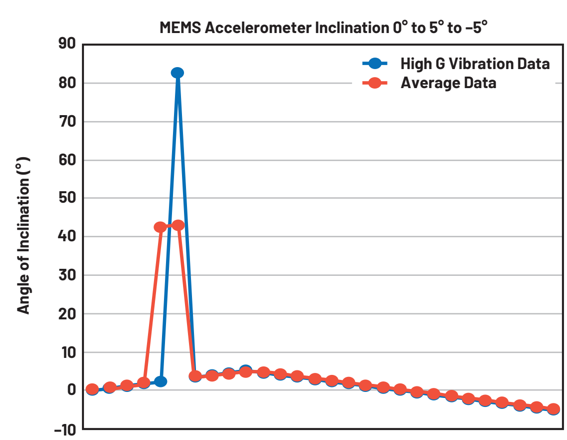

Figure 7. Inclination data with high g vibration present and averaged data.

While a momentary impact, shock, or vibration does not affect the actual tilt or inclination of a motor, the conversion process from acceleration to tilt presents these data as an actual tilt value as seen in Figure 7. Averaging the data or generating the mean is a common approach to remove such anomalies, and this is a feature of the Voyager platform GUI as seen in Figure 8.

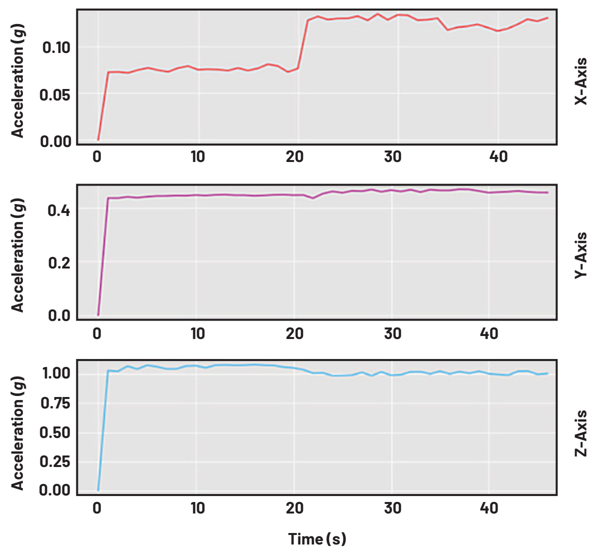

Figure 8. Mean vibration on three axes.

The measurement in Figure 8 shows the motor running from 1 s onward with 4° tilt applied at around 18 s. While some change can be observed on the y- and z-axes, the x-axis clearly detects the tilt. This is one of the key advantages of a 3-axis vibration sensor where, in this case, it is mounted to detect vibrations primarily on the z-axis, then the y-axis. The x-axis can detect the tilt more accurately as it is out of the axis for the vibration measurement. While the exact amount of tilt is difficult to determine with a high degree of accuracy under dynamic conditions, a simple characterization of the motor and allowable inclination range can yield good results. The tilt shown in Figure 8 works out as $\sin^{-1} 0.07\ g = 4°$ when the z-axis is measuring 3 *g*, y-axis 1.3 *g*, and x-axis 0.2 *g* as shown in Figure 9. The static tilt resolution of the Voyager module is about 0.2°.

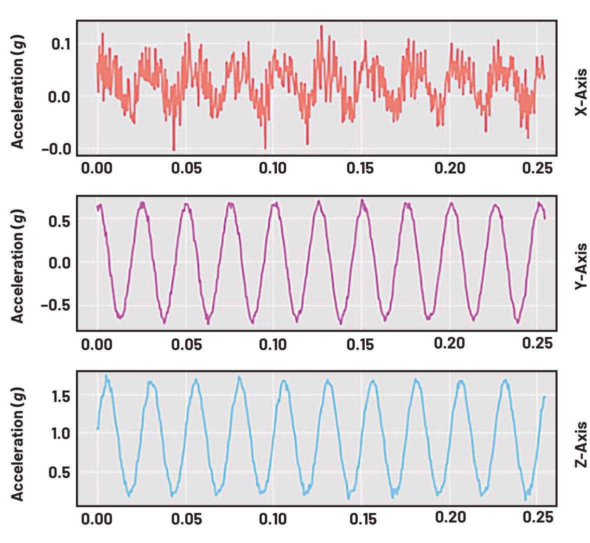

Figure 9. Time domain plots showing vibrations measured on three axes.

Another key data sheet parameter that needs to be considered when designing a MEMS-based wireless vibration module capable of detecting tilt is the *g*-range. If a MEMS sensor is exposed to vibrations that exceed the *g*-range, clipping can occur and this manifests itself as a DC offset, thereby adding error to any resulting tilt measurements. This means when selecting a MEMS sensor for detecting tilt in the presence of vibration, you must ensure that the *g*-range has headroom above any prospective shock, impact, or vibration event magnitudes to avoid this source of offset.

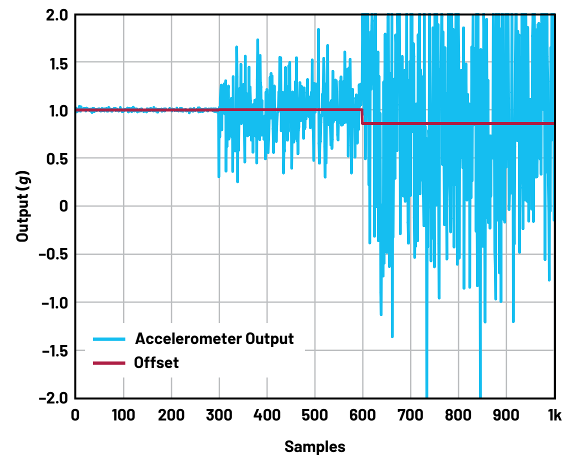

Figure 10. Vibration rectification in an accelerometer with ±2 g full-scale range due to asymmetric clipping.

Fault Detection Using Voyager

The ability of the Voyager triaxial vibration measurement solution to pick up faults and deliver insights is not possible with single-axis solutions. Fault detection based on vibration is a complex process in which many mathematical models and even AI are used to diagnose faults. Voyager-based results are intended to show how 3-axis measurements can be used to derive extra confidence and to provide a more robust method to diagnose specific faults when compared to a single-axis sensor.

Figure 11 shows the SpectraQuest lite rig, which provides the ability to perform controlled experiments on a device that emulates real-world machinery. An in depth understanding of fault signatures due to imbalance loads, cocked or eccentric rotors, bent rotor shafts, and damaged bearing/bearing housings can be simulated to achieve a better understanding of vibration signatures. The Voyager wireless mote is mounted on the housing as shown in Figure 11 and is well situated to measure both radial (z and y direction) vibration amplitudes, as well as axial vibration in the direction of the shaft and loads.

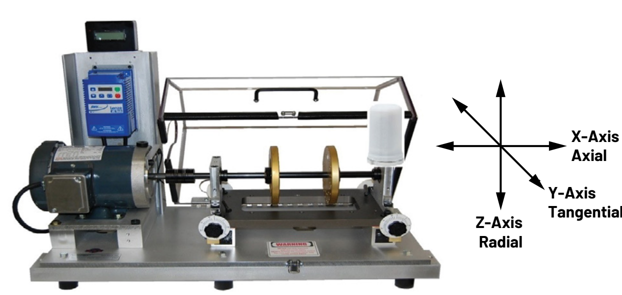

Figure 11. SpectraQuest lite rig.

Imbalance and Misalignment

Imbalance and misalignment are grouped together as both fault signatures, and they often show up in the same FFT analysis. An uneven distribution around the center of gravity of the motor's rotor, as shown in Figure 12, can lead to imbalance whereby the rotor vibrates and can put extra strain on the bearings. These vibrations can lead to excessive wear of the bearings, which in turn creates more noise and, if left unmaintained, can lead to failure of the bearings or even the entire motor.

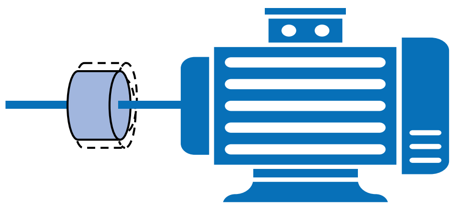

Figure 12. Uneven distribution of mass around an axis of rotation.

Rotor misalignment occurs when the rotor, coupling element, and driven shaft are not centered as shown in Figure 13. The misalignment can be angular, parallel, or a combination of the two. The most common vibration resulting from misalignment is at 1× rpm frequency. There is a possibility that the 2× rpm frequency can exceed the 1× frequency, but this is not common. It should be noted that a bent shaft and imbalance also produce vibrations at 1× rpm frequency.

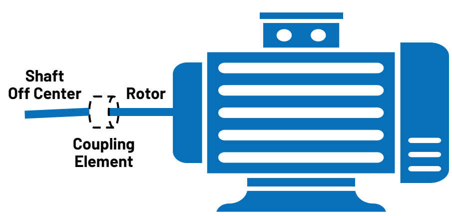

Figure 13. Centerlines of the rotor and the driven equipment shafts are not in line with each other.

Imbalanced Load

A system is potentially unbalanced if there is an increased vibration amplitude at the rotational rate (1×) compared to the baseline background vibration noise. To simulate imbalance, a load with added mass at its extremity was placed on the SpectraQuest rig shaft. The system was operated at 3000 rpm, and a 5 kg load was added. Figure 14 shows a clear increase in the 1× in the z radial direction compared to the baseline vibration as would be expected. Figure 15 presents an FFT analysis of vibration amplitude gathered across x-, y-, and z-axes. There's a clear increase in the 1× in y and z radial directions, but also a clear increase in the vibration amplitude at 9× and 10× rotational rates in the x axial direction, which would not be picked up with a single-axis sensor.

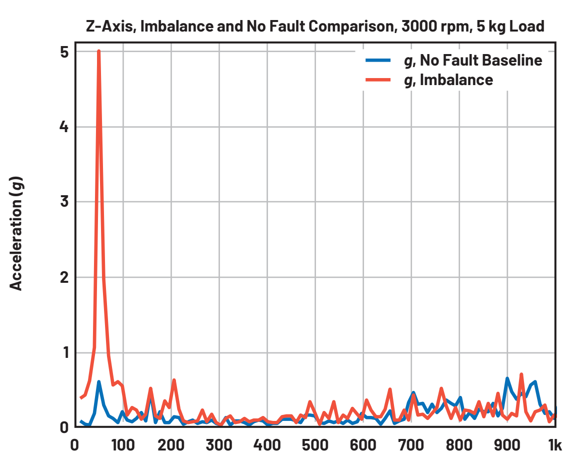

Figure 14. Imbalance FFT analysis at 3000 rpm with a 5 kg load, z-axis compared to baseline.

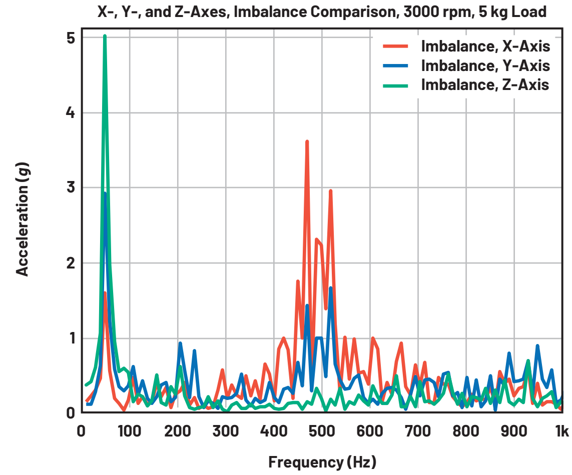

Figure 15. Imbalance FFT analysis at 3000 rpm with a 5 kg load.

Cocked Rotor

Figure 16 shows an FFT analysis for a cocked rotor (0.5° off axis) added to the SpectraQuest rig. The frequency spectrum shows a large increase in the vibration amplitude at the 1× rotational rate, but with also a repetitive increase in vibration amplitude at harmonics 3×, 4×, 5×, 6×, 7×, 8×, 9×, and 10× in the axial direction. Like the imbalanced load, the cocked rotor shows fault signatures in the axial direction, which would not be identified using a single-axis vibration sensor.

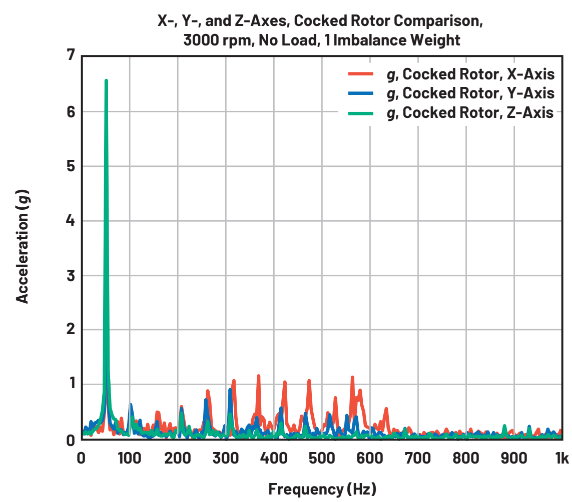

Figure 16. Cocked rotor FFT analysis at 3000 rpm with no load and one imbalance weight.

Eccentric Rotor

Figure 17 shows an FFT analysis for an eccentric rotor added to the SpectraQuest rig. The frequency spectrum shows a large increase in the 1× first harmonic, indicating imbalance in the radial (z) direction, but there is also a large increase in the 3× harmonic in the axial direction, indicating misalignment.[6,7] A 3-axis sensor will capture both misalignment and imbalance due to an eccentric rotor defect, which would obviously be missed with a single-axis sensor solution.

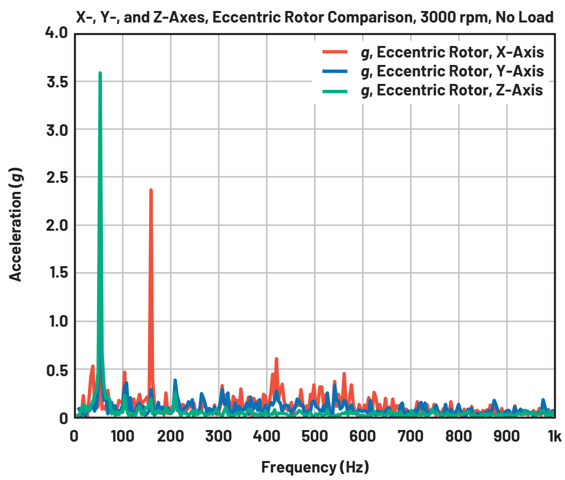

Figure 17. Eccentric rotor FFT analysis at 3000 rpm with no load.

Bent Shaft

Figure 18 shows an FFT analysis for a bent shaft added to the SpectraQuest rig. The frequency spectrum shows a large increase in the 1× first harmonic, indicating imbalance in both the radial (z) and (y) directions, but there is also a large increase in the 3× harmonic in the axial direction, indicating misalignment. The additional peak in the y direction at 1× helps to differentiate between the bent shaft and eccentric rotor simulated faults. A 3-axis sensor will capture both misalignment and imbalance due to a bent shaft, which would obviously be missed with a single-axis sensor solution.

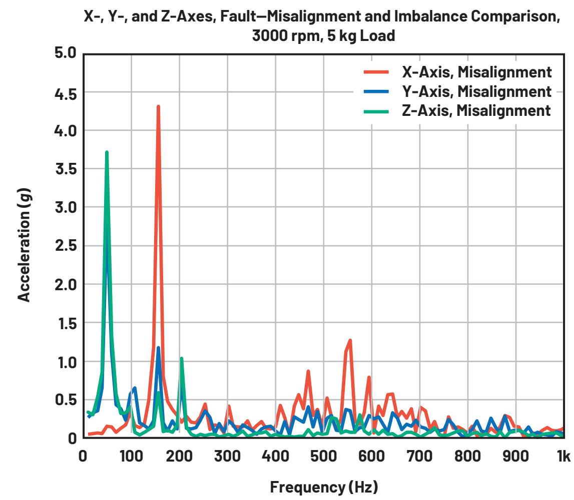

Figure 18. Bent shaft FFT analysis at 3000 rpm with no load.

Table 1 summarizes the most common machine faults, which show up at low frequency.

Bearing Defects

Based on bearing geometry, there are several fundamental calculated classifications of bearing defects. Ball pass frequency inner (BPFI) and ball pass frequency outer (BPFO) are the frequencies generated when rolling elements roll across a defect in the bearing outer or inner ring.

Table 1. Simulated Fault Description and Fault Signature

Fault Simulated	Load or Rotor Placed on the Shaft	Imbalance Fault Signature?	Misalignment Fault Signature?	Other Fault Signature?
Mass Imbalance—Unequal Distribution of Mass. Mass Added at Extremity of the Load.	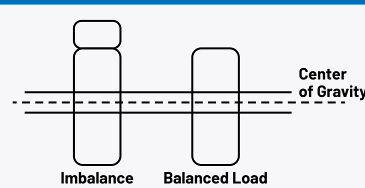	✓	✗	✗
Cocked Rotor. The Rotor Is 0.5° Off Axis.	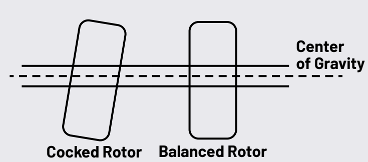	✓	✗	✓
Eccentric Rotor. The Rotor Is Off Center—Asymmetric Center Point When Placed on the Shaft.	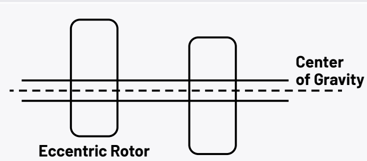	✓	✓	✗
Bent Shaft. Image Opposite Is Exaggerated for Illustration Purposes.	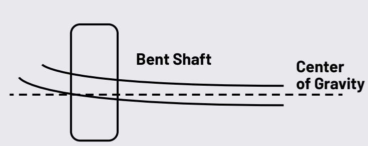	✓	✓	✗

Ball Pass Frequency Inner

A bearing with a defect in the inner ring was mounted to the SpectraQuest rig, with the shaft and loading securely attached through the defective bearing case. The BPFI can be calculated using

$$BPFI = \frac{N}{2} \times F \times \left(1 + \frac{B}{P}\right) \times cos\ \theta$$

where *F* is the frequency, *N* is the number of balls, *B* is the ball diameter, θ is the contact angle, and *P* is the pitch diameter. For the SpectraQuest rig, the user manual provides the calculation for you. Based on the eight rolling elements used in a 5/8" rotor bearing, with a rolling element diameter of 0.3125", and a pitch diameter of 1.318", the BPFI is calculated at 4.95× the fundamental rotation rate.

Figure 19 shows the Voyager sensor FFT analysis of the bearing defect inner ring fault on the SpectraQuest rig. The BPFI is picked up at approximately 250 Hz (~4.95×) on the y-axis (radial). It's worth noting that this is also on the z radial axis, but the vibration amplitude is not as large and pronounced.

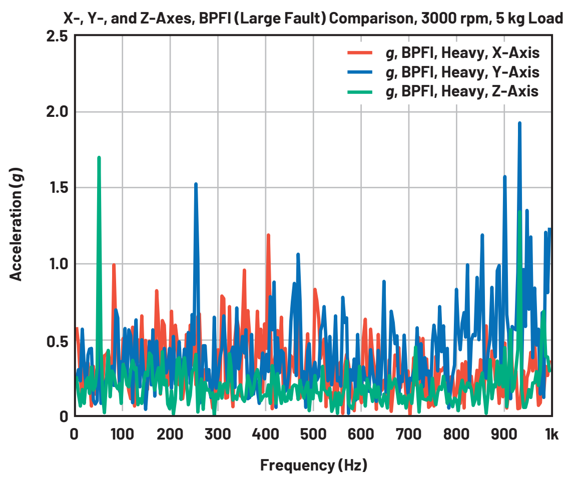

Figure 19. BPFI FFT analysis at 3000 rpm with a 5 kg load.

Ball Pass Frequency Outer

A bearing with a defect in the outer ring was mounted to the SpectraQuest rig, with the shaft and loading securely attached through the defective bearing case. The BPFO can be calculated using

$$BPFO = \frac{N}{2} \times F \times \left(1 - \frac{B}{P}\right) \times cos\ \theta$$

For the SpectraQuest rig, the user manual provides the calculation for you. Based on the eight rolling elements used in a 5/8" rotor bearing, with a rolling element diameter of 0.3125", and a pitch diameter of 1.318", the BPFO is calculated at 3.048× the fundamental rotation rate.

Figure 20 shows the Voyager sensor FFT analysis of the bearing defect outer ring fault on the SpectraQuest rig. The BPFO is picked up at approximately 150 Hz (~3.048×) on the y and z radial axes. It's worth noting that this defect does not show as a large amplitude at the BPFO 3.048× estimated signature when compared to the 4.95× BPFI estimated signature.

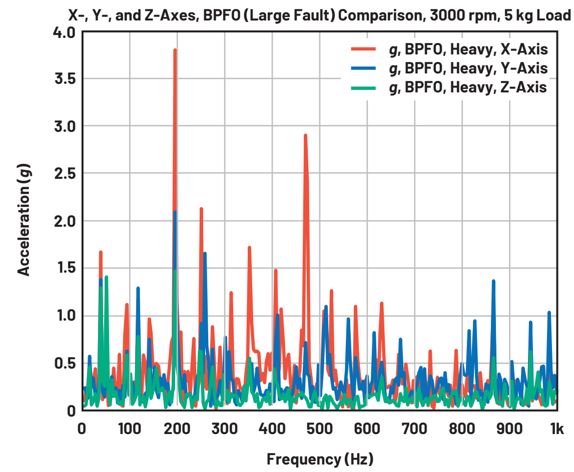

Figure 20. BPFO FFT analysis at 3000 rpm with a 5 kg load.

Diagnosing Faults: How to Use Fault Signatures in Algorithms

Table 2 shows that the triaxial Voyager vibration sensor picks up fault signatures in the axial direction, which can be used to distinguish between specific faults. For example, both eccentric and cocked rotor faults result in a large increase in vibration amplitude at the system rotational rate (1×). However, in the axial direction, an eccentric rotor shows an increase in the 3× harmonic only, but the cocked rotor shows an increase in 3×, 4×, and so on up to 10× harmonics. These simple patterns in frequency harmonics can be used in an algorithm to distinguish between the two faults. The Voyager triaxial solution provides insights, which are clearly not possible with a single-axis solution.

Another example is the ability to distinguish between an imbalanced load and a bent shaft. Both an imbalanced load and a bent shaft will result in an increase in the vibration amplitude at the system rotational rate (1×). This 1× increase will occur radially (in both vertical and horizontal directions). However, in the axial direction, the imbalanced load will result in an increase in the 9× and 10× harmonics, but in comparison, a bent shaft will show an increase in the 3× harmonic (misalignment signature).

As noted earlier, the bent shaft and eccentric rotor defects can be differentiated by the large increase in the radial (y) direction for the bent shaft, which is not present in the eccentric rotor test.

For bearing faults, the Voyager triaxial solution picks up the BPFI in the radial horizontal (y) direction, but not the vertical radial direction (z). If a single-axis solution is used, then this bearing inner race fault will not be detected, unless the user is lucky enough to correctly guess the axis where *g* amplitude is greatest.

Table 2. Summary of Fault Frequency Signatures for Commonly Occurring Machine Faults

Fault	Fault Signature on Axis and Commonly Occurring Fault Frequency (1× or Multiple of Fundamental Rotation Rate)		
	Z-Axis (Radial—Vertical)	Y-Axis (Radial—Horizontal)	X-Axis (Axial)
Imbalance Load	1×	1×	9×, 10×
Eccentric Rotor	1×		3×
Cocked Rotor	1×		3×, 4×, 5×, 6×, 7×, 8×, 9×, 10×
Bent Shaft	1×	1×	3×
BPFO (Bearing Rolls Across Defect in Outer Race)	3× (BPFO), 4×	3× (BPFO), 4×	
BPFI (Bearing Rolls Across Defect in Inner Race)	1×	5× (BPFI)	

Conclusion

Recent advancements in MEMS capabilities have seen a rapid rise in their use for CbM, but there still exists some ambiguity about their capabilities, which are extremely varied. This article outlined the capabilities of triaxial MEMS sensors suitable for CbM vs. higher performance, single-axis MEMS, and piezo/IEPE sensors to clarify exactly what different sensors are capable of. While piezo sensors typically have lower noise at higher frequencies, MEMS can offer lower noise close to 0 Hz, which suits a lot of CbM applications. This capability coupled with three sensing axes can even be extended to coarse tilt detection in the presence of vibration, useful for detecting soft foot issues.

Various faults were seeded on a test rig which the triaxial MEMS sensor in the Voyager module was clearly able to detect such as imbalance, misalignment, bearing issues, cocked rotor, and bent shaft. Furthermore, the confidence that a triaxial sensor can provide in identifying specific faults also adds merit to triaxial MEMS sensor use in vibration measurement systems for CbM.

In Part 3 of this article series, we will investigate different power modes of the Voyager module as well as discussing the power and software architecture and how they can be managed to optimize performance.

References

[1] "Unplanned Downtime in Numbers: How Bad Is It?" Intech Automation Intelligence, April 2021.

[2] Brian Graney and Ken Starry. "Rolling Element Bearing Analysis." *Materials Evaluation*, Vo. 70, pp. 78–85, 2011.

[3] "Eddy Current Principle NCDT." Micro-Epsilon.

[4] Bjorn Ryden. "Predictive Maintenance with Vibration Sensors." TE Connectivity, 2021.

[5] "Low Frequency Machinery Monitoring: Measurement Considerations." Wilcoxon Sensing Technologies.

[6] R. Keith Mobley. *An Introduction to Predictive Maintenance*. Butterworth-Heinemann, 2002.

[7] "Unlocking Performance." IndustryWeek and Emerson.

[8] Olav Vaag Thorsen and Magnus Dalva. "A Survey of Faults on Induction Motors in Offshore Oil Industry, Petrochemical Industry, Gas Terminals and Oil Refineries." Proceedings of IEEE Petroleum and Chemical Industry Technical Conference (PCIC '94), 1994.

About the Authors

Richard Anslow is a system applications engineer with the Connected Motion and Robotics Team within the Automation and Energy Business Unit at Analog Devices. His areas of expertise are condition-based monitoring and industrial communication design. He received his B.Eng. and M.Eng. degrees from the University of Limerick, Limerick, Ireland. He can be reached at richard.anslow@analog.com.

Chris Murphy is an applications engineer with the European Centralized Applications Center, based in Dublin, Ireland. He has worked for Analog Devices since 2012, providing design support on motor control and industrial automation products. He holds a Master of Engineering in electronics by research and a Bachelor of Engineering in computer engineering. He can be reached at chris.murphy@analog.com.